

Journal of Materials Chemistry

Supporting Information

A Facile and Efficient Strategy for the Preparation of Stable CaMoO₄ Spherulites Using Ammonium Molybdate as a Molybdenum Source and Their Excitation Induced Tunable Luminescent Properties for Optical Applications

G. Seeta Rama Raju, E. Pavitra, Yeong Hwan Ko, and Jae Su Yu*

Department of Electronics and Radio Engineering, Kyung Hee University, 1 Seocheon-dong, Giheung-gu, Yongin-si, Gyeonggi-do 446-701 Republic of Korea

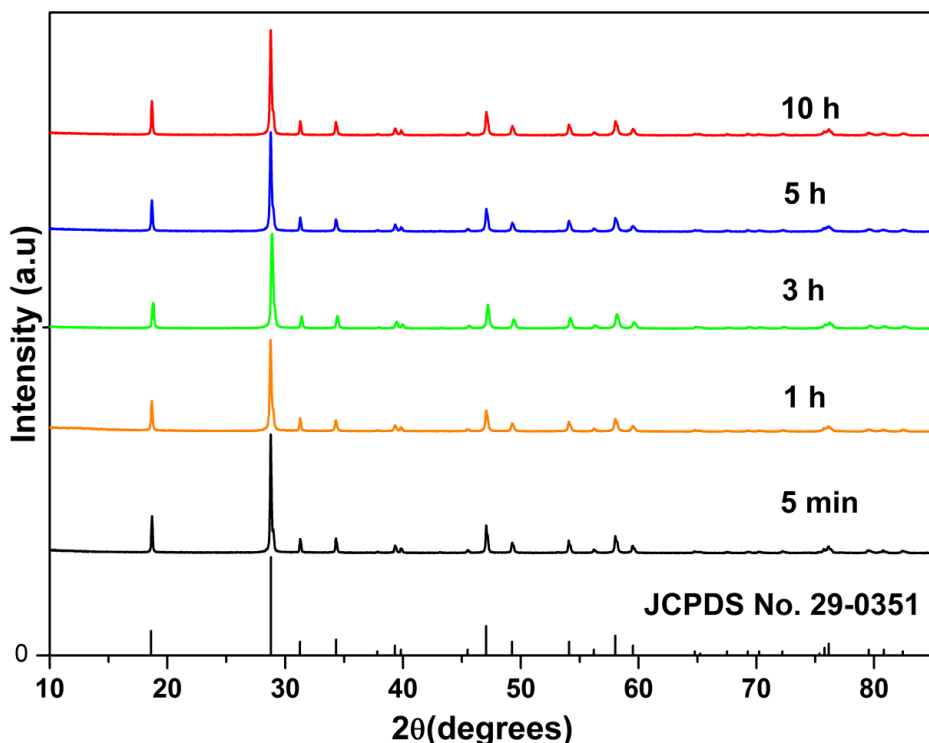


Fig. S1. XRD patterns of the CaMoO₄ samples prepared at 160 °C for different reaction times

The XRD patterns are in well agreement with the JCPDS No. 29-0351 without any impurity phase, which confirms that the prepared samples have scheelite based tetragonal structure. From the XRD patterns, it is clear that the intensity of the diffraction peaks decreases with increased full width at half maximum (FWHM) when the reaction time increases from 5 min to 1 h, and above 1 h the intensity of diffraction peaks increases. Furthermore, the intensity

of the diffraction peaks almost the same for the reaction times of 5 and 10 h. It indicates that the metastability was confirmed between 3 and 5 h of reaction time and which was also confirmed by the SEM image of Fig. 1(d), where the growth was extended in different directions for 5 h of reaction time.

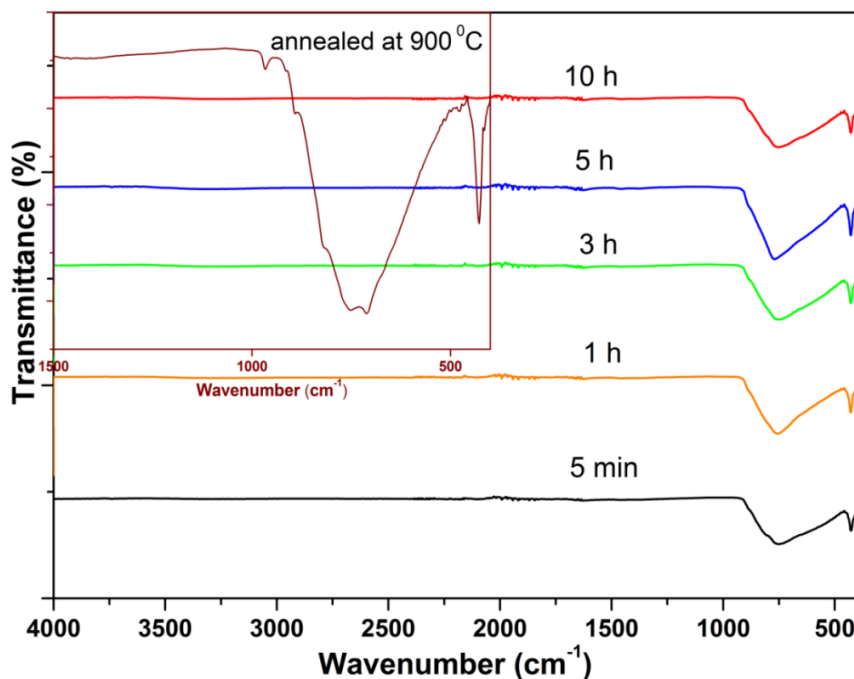


Fig. S2. FTIR spectra of the CaMoO₄ samples prepared at 160 °C for different reaction times
(Inset shows the FTIR spectrum of the sample annealed at 900 °C)

The FTIR spectra of the CaMoO₄ nanostructures prepared at 160°C with different reaction times have been shown in Fig. S2. First of all, there appear no absorption bands that are characteristic of OH groups in scheelite structure, indicative of successful formation of the tetragonal phase in our samples without OH contamination, which is a good sign for expecting high quality CaMoO₄ nanostructures. Generally, in the case of scheelite structure, the internal mode vibrations of F₂(v₃) and F₂(v₄) corresponding to the respective anti-symmetric stretching and bending vibrations are active.^[1] The IR spectrum showed that the broad band between 460

and 910 cm^{-1} with band maxima from 750 to 780 cm^{-1} of CaMoO_4 phase, which is related to the Mo-O anti-symmetric stretching vibrations of MoO_4^{2-} for the $\text{F}_2(\nu_3)$ vibrations.^[2] The other sharp peak observed at 428 cm^{-1} is associated with the $\text{F}_2(\nu_4)$ internal modes due to the presence of anti-symmetric bending vibrations involved in the O-Mo-O bonds.^[3] The position of the stretching vibrations depends upon the several factors such as crystallite size, mass, and radii of the cation.^[4, 5] The overlapped figure shows the FTIR spectra of the sample annealed at $500\text{ }^\circ\text{C}$, which shows the multiple splittings of stretching vibrations, meanwhile the band shift towards the higher frequency. This indicates that the crystalline order increases with raising the reaction time and annealing temperature as a result the interaction forces between O-Mo-O increases.^[6]

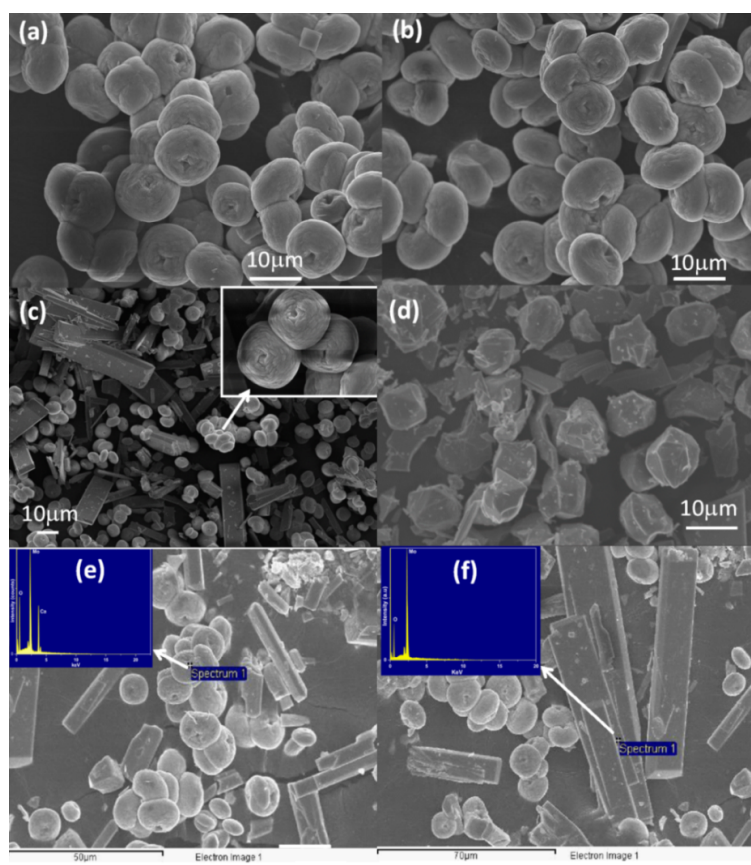


Fig. S3. (a), (b) and (c) SEM images at different places of the CaMoO₄ prepared at 160 °C for 10 h of reaction time (d) SEM image of the sample annealed at 500 °C for 5 h (e) EDAX for the erythrocyte like morphology, and (f) EDAX for the rod/plate like morphology.

The erythrocyte like morphology of CaMoO₄ was prepared using hydrothermal synthesis, but it is only possible when mixed with 1 mol Ca(NO₃)₂ and 1 mol (NH₄)₆Mo₇O₂₄. In this case the molybdenum rich CaMoO₄ has been formed and the excess of the molybdenum was sticked on the walls over the solvent. The reason is that in the hydrothermal synthesis heptamolybdate undergoes fragmentation into smaller units such as MoO₄ and MoO₆ under slightly acidic condition. These smaller fragments of MoO₄²⁻ can react with Ca²⁺ and excess of MoO₆⁶⁻ clusters are separately formed like rods, which can be clearly observed in the EDAX images. This type of formation is not completely stable because the equilibrium species will change when the aqueous molybdate solution is subjected to hydrothermal treatment. The results reported here suggest that the Mo concentration play a crucial role on the formation of stable CaMoO₄.

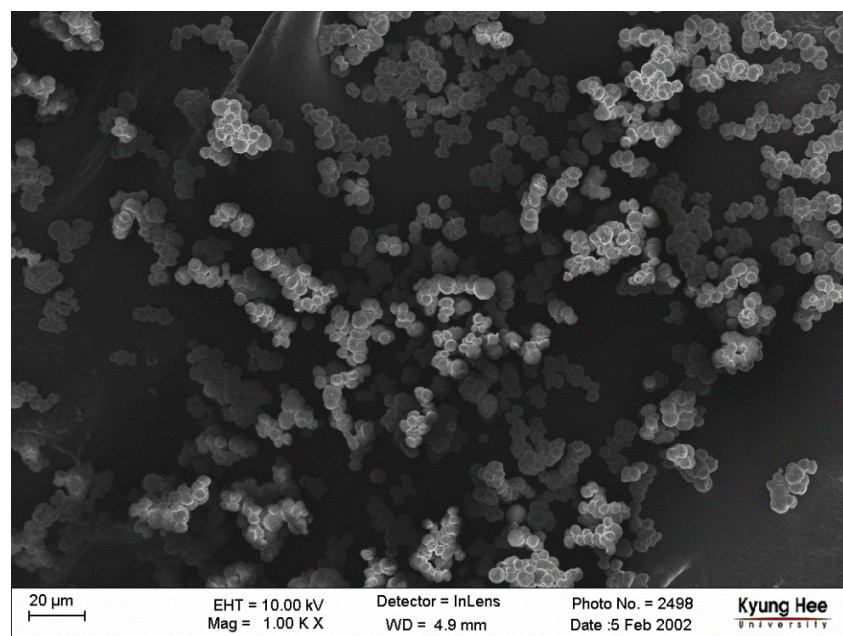


Fig. S4: Low resolution SEM image of the mono dispersed spherulites annealed at 900 °C

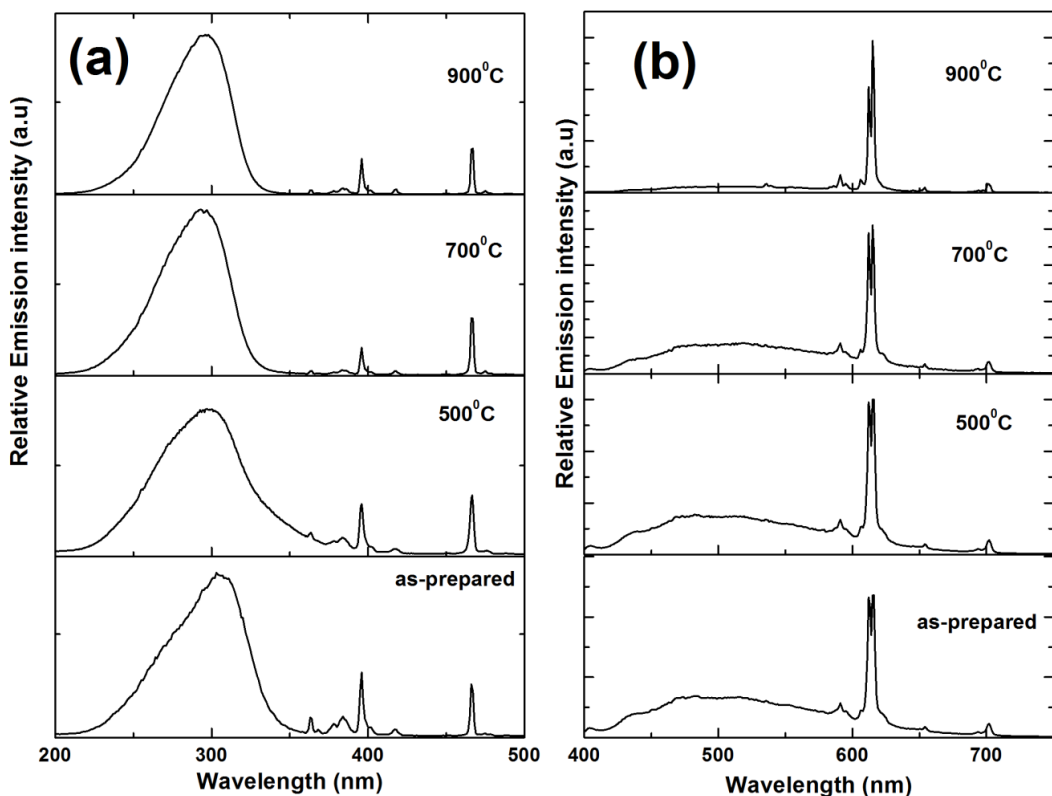


Fig. S5. (a) Excitation and (b) Emission spectra of CaMoO₄: Eu³⁺ at different annealing temperatures.

Fig. S5(a) shows the photoluminescence excitation (PLE) spectra for the CaMoO₄: 5 mol% Eu³⁺ samples annealed at different temperatures, by monitoring the emission wavelength at 614 nm. The both PLE spectra reveal the broad excitation band also called charge transfer band (CTB), which is due to the charge transfer between the completely filled 2p orbital of O²⁻ ion and the partially filled 4f orbital of the Eu³⁺ ion and the position of this band depends strongly on the host lattice. This CTB is overlapped with the Mo-O CTB in the shorter wavelength region, and it also consists of sharp excitation bands in the longer wavelength region due to the f-f transitions of Eu³⁺ ion. The overlapping of both CTB indicates the possibility of white light emission. The sharp excitation peaks is due to intra-configurational f-f transitions of Eu³⁺ ions are assigned to the electronic transitions of (⁷F₀→⁵D₄) at 362 nm, (⁷F₀→⁵G₃) at 376

nm, ($^7F_0 \rightarrow ^5G_4$) at 382 nm, ($^7F_0 \rightarrow ^5L_6$) at 396 nm, ($^7F_0 \rightarrow ^5D_3$) at 412 nm, ($^7F_0 \rightarrow ^5D_2$) at 466 nm. These Eu³⁺ sharp excitation peaks indicate that violet and blue laser diodes/LEDs are efficient pumping sources in obtaining Eu³⁺ emissions.

It is worthy to note from Fig. S5(a) that the intensities of CTB at around 300 nm were higher than that of ($^7F_0 \rightarrow ^5L_6$) transition at 396 nm and the intensity of ($^7F_0 \rightarrow ^5L_6$) higher than ($^7F_0 \rightarrow ^5D_2$) at 466 nm of Eu³⁺ ions for the as-prepared samples (CTB > 396 nm > 466 nm). While increasing the annealing temperature from 500 to 900 °C the broadness (or strength) of the CTB increases and the band maxima shift towards the higher energy side. In the longer wavelength region the intensity of ($^7F_0 \rightarrow ^5D_2$) at 466 nm increases as compared to ($^7F_0 \rightarrow ^5L_6$) at 396 nm, which indicate that the quantum efficiency of Eu³⁺ increases with increasing the annealing temperature. The increase of intensity in the visible wavelength region is a good sign for the development of tri color based white LEDs. The CTB is related to the stability of the electron of the surrounding O²⁻ ion i.e., the CT transition is sensitive to a ligand environment (the bonding energy between the central ion and the ligand ions). The fact that it occurs in the solid state (ionic oxides) is explained by the strong potential field at the anion (O²⁻) sites due to the surrounding ions. If this potential increases, the energy required transferring an electron from the O²⁻ ion to the cation (Eu³⁺) also increases, and the CTB moves to higher energy side.^[7-9] In nanoscale samples, especially very tiny ones, the Eu-O distance is long, indicating that the Eu-O bonds become weaker, less covalent and high ionicity, which weakens the binding energy of an electron to O²⁻. Therefore, the electron needs less energy to transfer from O²⁻ to Eu³⁺, resulting in the CTB placed in the lower energy region. On the other hand, as particle size increases the surface to the volume ratio decreases and Eu-O distance is short. As a result, it requires more energy to remove an electron from an O²⁻ ion; therefore, the CTB shifted towards higher energy.

These results are also consistent with the Hoefdraad's study on the CTB of Eu³⁺ in oxides, where he concluded that the CTB band position of Eu-doped oxide depends on the bond length of Eu-O and the coordination environment around Eu³⁺.^[10] Note that the variation of the CTB described in different literatures is quite incompatible. For example, in Y₂O₃:Eu³⁺ nanocrystals, some authors observed a blue shift whereas the others observed a red shift.^[8, 11] As it is well known, the resonant excitation cross-sections of f-f transitions for trivalent rare earth ions are generally small and play an important role in the excitation of Eu³⁺ ions.

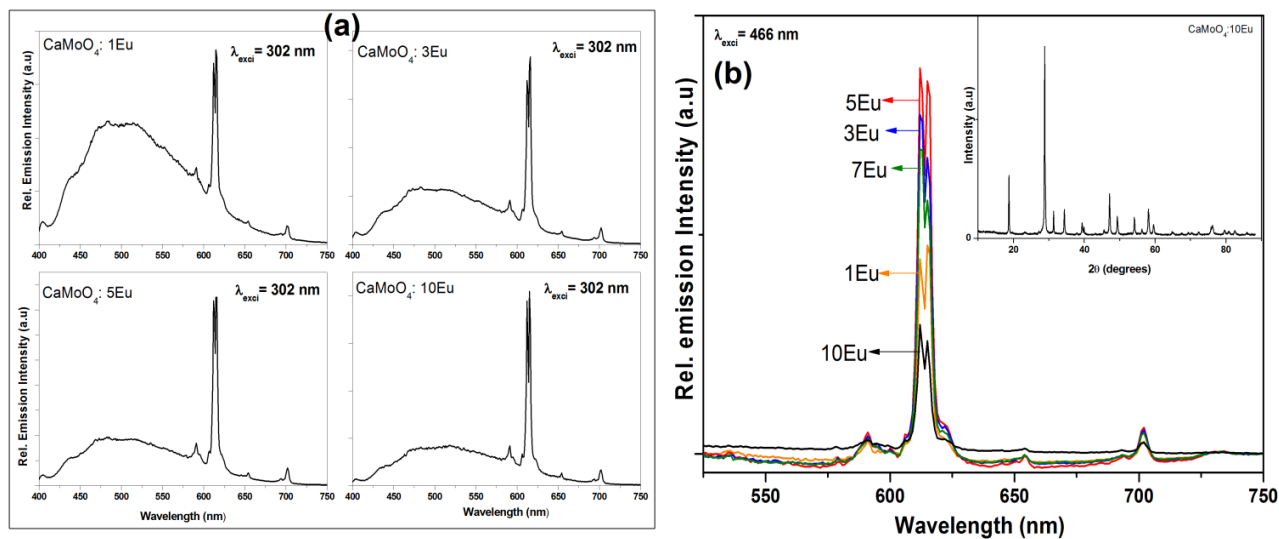


Fig. S6. Emission spectra of CaMoO₄ when doping with different concentrations of Eu³⁺ ions (a) excited at 302 nm, and (b) excited at 466 nm

Fig. S6(a) shows the occurrence of efficient energy transfer from Mo-Eu by exciting at 302 nm for different Eu³⁺ concentrations. In Fig. S6(b), the emission spectra shows only (⁵D₀) Eu³⁺ transitions when exciting with 462 nm, which are similar for different Eu³⁺ concentrations. When the Eu³⁺ concentration increases from 1 to 5 mol% the emission intensity also increases and the Eu³⁺ concentration further increases above 5 mol% the emission intensity decreases due to the concentration quenching. The concentration quenching might be elucidated by the

following two factors: (i) the excitation migration due to the resonance between the activators is enhanced when the doping concentration is increased, and thus the excitation energy reaches quenching centers, and (ii) the activators are paired or coagulated and are changed to quenching center. Moreover, the asymmetric ratio increases with increasing the concentration of Eu^{3+} clearly observed in Fig. S6(b). A.K. Parchur et al.^[12] reported that CaMoO_4 shows the impurity peaks in the XRD patterns when doping with 10 mol% Eu^{3+} ions. However, in the present work no impurity phases were observed upto 10 mol% of Eu^{3+} ions doped into Ca sites as shown in the inset of Fig. S6(b).

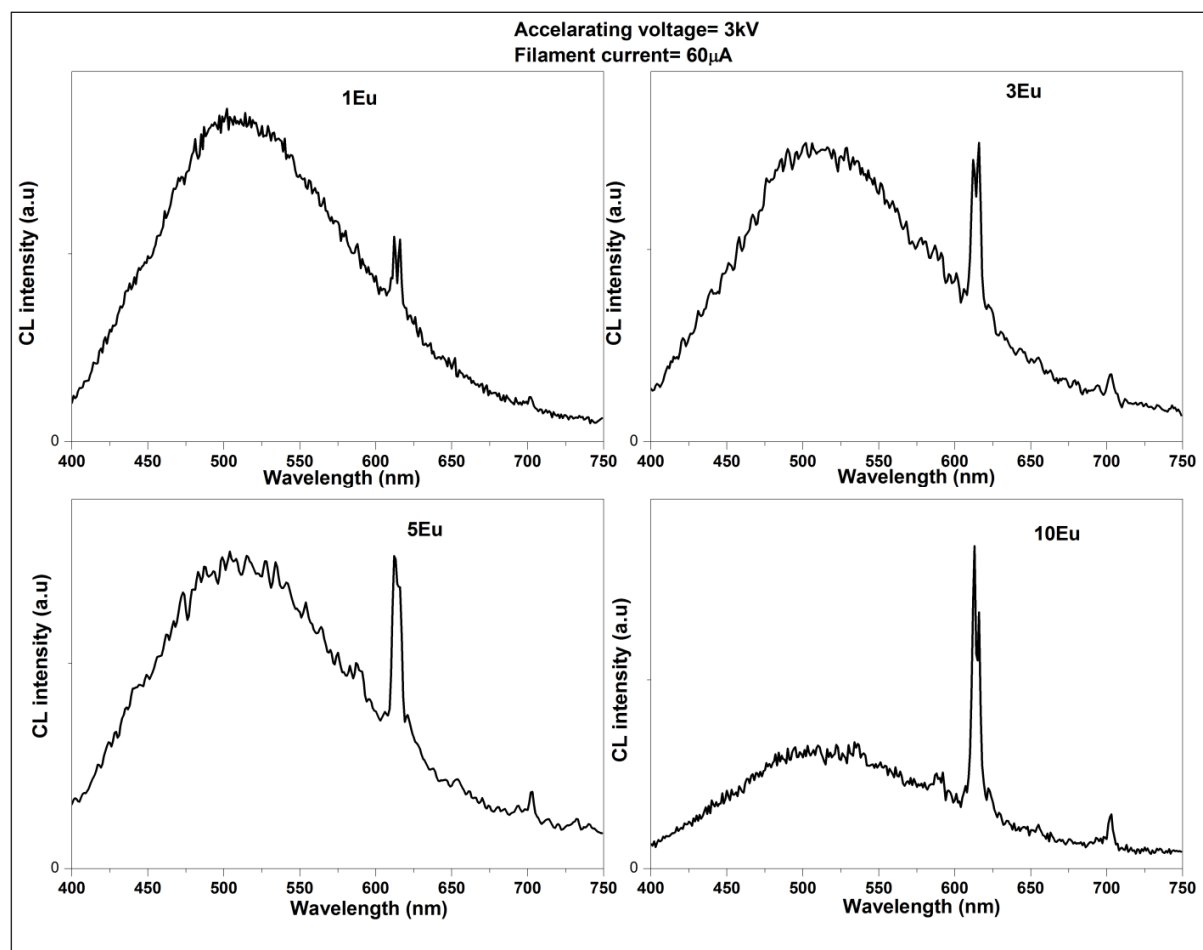


Fig. S7. CL spectra of CaMoO_4 when doping with different concentrations of Eu^{3+} ions

Table S1: *CIE chromaticity coordinates calculated from the PL spectra of the CaMoO₄ samples doped with different concentrations of Eu³⁺ ions prepared at 160 °C for 10 h of reaction time*

Concentration Of Eu ³⁺ (mol%)	CIE chromaticity coordinates		
	$\lambda_{\text{exc}} = 302 \text{ nm}$	$\lambda_{\text{exc}} = 396 \text{ nm}$	$\lambda_{\text{exc}} = 466 \text{ nm}$
1	(0.295, 0.368)	(0.594, 0.405)	(0.59, 0.409)
3	(0.323, 0.359)	(0.602, 0.397)	(0.599, 0.4002)
5	(0.339, 0.359)	(0.606, 0.394)	(0.603, 0.396)
7	(0.342, 0.362)	(0.602, 0.388)	(0.622, 0.382)
10	(0.338, 0.386)	(0.602, 0.398)	(0.651, 0.348)

Table S2: *CIE chromaticity coordinates calculated from the CL spectra of the CaMoO₄ samples doped with different concentrations of Eu³⁺ ions prepared at 160 °C for 10 h of reaction time*

Concentration Of Eu ³⁺ (mol%)	CIE chromaticity coordinates	
	Accelerating voltage=3 kV & Filament current= 60 μA	
0		(0.282, 0.387)
1		(0.289, 0.87)
3		(0.303, 0.385)
5		(0.331, 0.379)
7		(0.344, 0.379)
10		(0.369, 0.389)

References:

- [1] V. C. Farmer, M. Society, *The infrared spectra of minerals*, Mineralogical Society London, 1974.
- [2] A. P. A. Marques, F. V. Motta, E. R. Leite, P. S. Pizani, J. A. Varela, E. Longo, D. M. A. de Melo, *J. Appl. Phys.* 2008, **104**, 043505.
- [3] L. Hechang, Z. Xuebin, Z. Shoubao, L. Gang, T. Xianwu, S. Wenhai, Y. Zhaorong, D. Jianming, S. Yuping, *J. Phys. D: Appl. Phys.* 2009, **42**, 045404.
- [4] T. T. Basiev, A. A. Sobol, Y. K. Voronko, P. G. Zverev, *Opt. Mater.* 2000, **15**, 205.
- [5] A. Marques, E. Leite, J. Varela, E. Longo, *Nanoscale Res. Lett.* 2008, **3**, 152
- [6] V. S. Marques, L. S. Cavalcante, J. C. Sczancoski, A. F. P. Alcântara, M. O. Orlandi, E. Moraes, E. Longo, J. A. Varela, M. Siu Li, M. R. M. C. Santos, *Cryst. Growth Des.* 2010, **10**, 4752.
- [7] G. Blasse, *J. Chem. Phys.* 1966, **45**, 2356.
- [8] T. Igarashi, M. Ihara, T. Kusunoki, K. Ohno, T. Isobe, M. Senna, *Appl. Phys. Lett.* 2000, **76**, 1549.
- [9] Z. Qi, M. Liu, Y. Chen, G. Zhang, M. Xu, C. Shi, W. Zhang, M. Yin, Y. Xie, *J. Phys. Chem. C* 2007, **111**, 1945.
- [10] H. E. Hoefdraad, F. M. A. Stegers, G. Blasse, *Chem. Phys. Lett.* 1975, **32**, 216.
- [11] Z. Qi, C. Shi, W. Zhang, T. Hu, *Appl. Phys. Lett.* 2002, **81**, 2857.
- [12] A. K. Parchur, R. S. Ningthoujam, S. B. Rai, G. S. Okram, R. A. Singh, M. Tyagi, S. C. Gadkari, R. Tewari, R. K. Vatsa, *Dalton Trans.* 2011, **40**, 7595.